THE JOURNAL OF PHYSICAL CHEMISTRY C

Article

pubs.acs.org/JPCC

Electronic and Structural Properties of BC_3 Nanotubes with Defects

Seifollah Jalili,*[,†,‡] Mojdeh Akhavan,[‡] and Jeremy Schofield[§]

[†]Department of Chemistry, K. N. Toosi University of Technology, P.O. Box 15875-4416, Tehran, Iran

[‡]Computational Physical Sciences Research Laboratory, School of Nano-Science, Institute for Research in Fundamental Sciences (IPM), P.O. Box 19395-5531 Tehran, Iran

[§]Chemical Physics Theory Group, Department of Chemistry, University of Toronto, 80 Saint George Street, Toronto, Ontario, Canada M5S 3H6

ABSTRACT: Defects, which naturally occur in nanostructures such as nanotubes, have a profound effect on their structure and electronic properties, and it is important to include them in the computational studies involving these nanotubes. In this Article, density functional theory calculations are utilized to investigate the impact of topological Stone-Wales (SW) and vacancy defects on the structural and electronic properties of a zigzag BC_3 nanotube. It is demonstrated that the most stable state for a SW defect is the structure in which an axial C−C bond is rotated by 90°. For vacancies at carbon sites, two possible configurations are obtained that are both nonmagnetic, whereas vacancy at a boron site induces magnetization in the structure of nanotube. The reconstruction of the boron vacancy can produce different kinds of defect states in the band gap of a semiconducting BC_3 nanotube, which are studied using band structure and density of states diagrams.

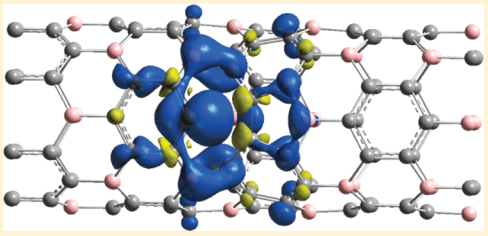

INTRODUCTION

Carbon nanotubes (CNTs), obtained by rolling up a hexagonal graphene sheet, are a class of 1D nanostructures with many interesting properties that make them promising materials for various technologies, such as energy storage, sensing, composites, and so on. In addition to pure graphitic sheets, compound sheets of boron, carbon, and nitrogen atoms have been produced experimentally.[1,2] These BCN monolayers, with atomic compositions such as BN, BC_2N, and BC_3, have a range of electronic behavior that can be tuned for specific applications.[3]

The existence of BC_3 nanotubes has been confirmed both experimentally using arch-discharge methods[4] and by first-principles and tight-binding calculations.[5] There is experimental[6,7] and theoretical[7] evidence that BC_3 nanodomains can be formed in a 1D nanotube structure upon boron substitution in CNTs. These studies show that BC_3 nanotubes are as likely to form as CNTs, with relative stabilities that are comparable to those of CNTs.

Many theoretical methods have been utilized to study the structural and electronic properties of BC_3 nanotubes.[5,8−10] Like CNTs, the electronic properties of BC_3 nanotubes can be understood from the folding of a planar sheet of BC_3. In Figure 1a, the fundamental lattice vectors of a BC_3 sheet are shown. The C−C and B−C bond lengths, calculated using local-density-approximation (LDA) scheme, are 1.42 and 1.55 Å, respectively. BC_3 sheets, as well as the resulting $(n, 0)$ zigzag and (n, n) armchair BC_3 nanotubes, are shown to be small-gap semiconductors.[5]

Similar to other nanotubes, the experimentally available BC_3 nanotubes may have some imperfections that are introduced either during their synthesis or as a result of applied stress.[11]

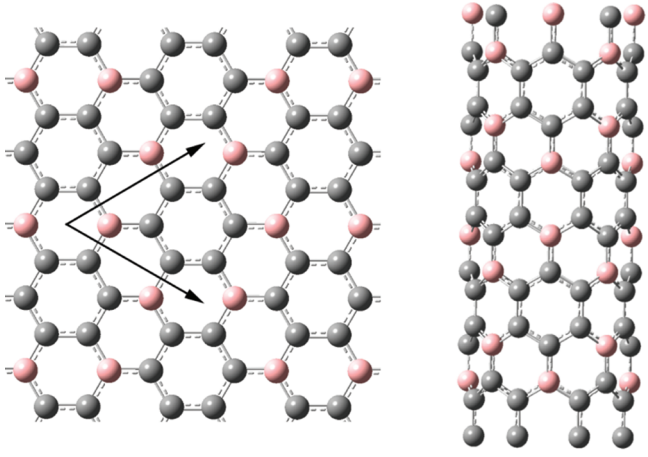

(a) (b)

Figure 1. Structure of a BC_3 sheet showing the hexagonal lattice vectors (a) and a (4, 0) BC_3 nanotube (b).

These defects, such as vacancies, antisites, and topological defects, alter the electronic, mechanical, and optical properties of nanotubes. Stone-Wales (SW) topological defects[12] (obtained by rotation of a chemical bond by 90°) and vacancies have been extensively studied in CNTs[13−16] and boron nitride nanotubes (BNNTs).[16,17] In this Article, the effects of SW defects, as well as carbon (V_C) and boron (V_B) vacancies on the structure and electronic properties of a zigzag

Received: April 3, 2012
Revised: May 17, 2012
Published: May 30, 2012

   dx.doi.org/10.1021/jp303184q | J. Phys. Chem. C 2012, 116, 13225−13230

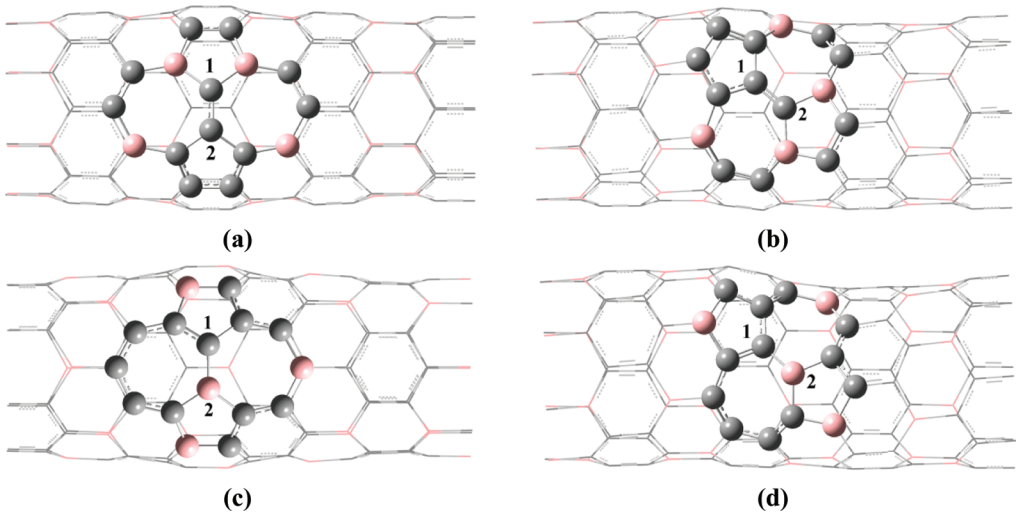

Figure 2. Optimized geometries for BC_3 nanotubes with a SW defect: SW-CC-a (a), SW-CC-c (b), SW-BC-a (c), and SW-BC-c (d).

BC_3 nanotube, are explored using density functional theory (DFT) calculations. The analysis of the electronic properties of BC_3 nanotubes with defects, in addition to studies on the mechanical behavior,[18] the barrier for Li diffusion[19] in BC_3 nanotubes, and the effect of radial deformation on electronic properties of BC_3 nanotubes,[8−10] is helpful to understand the properties and potential uses of these new materials in emerging technologies.

COMPUTATIONAL METHODS

DFT calculations were performed using plane-wave basis set and ultrasoft pseudopotentials,[20] implemented in the QUANTUM ESPRESSO package.[21] The generalized gradient approximation (GGA) with the Perdew−Burke−Ernzerhof (PBE) functional[22] was used using a plane-wave cutoff of 500 eV.

A BC_3 nanotube was made from a (8, 0) CNT by replacing appropriate carbon atoms with boron (Figure 1). Four unit cells were chosen along the tube axis to avoid the interaction between the defects and their 1D periodic images. The resulting nanotube had a length of 17.08 Å and 128 atoms, of which 32 atoms were B. Because the unit cell of a BC_3 sheet is about four times larger than that of the graphene sheet, a (n, m) BC_3 nanotube has a diameter close to a ($2n$, $2m$) CNT.[5] Therefore, a (4, 0) BC_3−NT is obtained from a (8, 0) CNT. The nanotube was placed in a tetragonal supercell of 20 Å × 20 Å × 17.08 Å to simulate an infinitely long 1D periodic system. The empty space along the lateral direction was included to avoid interactions in the xy plane.

Carbon (V_C), and boron (V_B) vacancies were created by removing one atom from the sidewall of the nanotube. An SW topological defect was created by rotating a bond in the nanotube by 90°, resulting in two heptagons with a common bond and two pentagons separated by a bond (i.e., a 5−77−5 arrangement). Four types of SW defects are possible in a zigzag BC_3 nanotube in which an axial (parallel to tube axis) or a circumferential (slanted) C−C or B−C bond is rotated. These are denoted by SW-CC-a, SW-CC-c, SW-BC-a, and SW-BC-c in Figure 2.

The tubes with defects were fully relaxed using the convergence threshold of 0.001 meV in energy and 0.003 eV/Å in force. For vacancy defects, spin-polarized calculations were utilized. The Brillouin zone sampling was performed using the gamma point for relaxation and a 1 × 1 × 7 Monkhorst-Pack[23] grid of k points for the calculation of energy and other properties. For band structure calculations, 11 k points were used along the Γ−Z direction. The optimized structures, after correcting the supercell length along the nanotube axis, were used to calculate various properties, such as the defect formation energy, band structure, and the density of states (DOS).

RESULTS AND DISCUSSION

A. Stone-Wales Defects. Optimized structures for BC_3 nanotubes containing a SW defect are shown in Figure 2. The nanotubes are rearranged to conform to the newly formed 5−77−5 ring system. As a result, the tube diameter near the defect position increases by ∼1 Å. Figure 2 shows that in the case of circumferential bond rotation (SW-CC-c and SW-BC-c systems), the deformation of nanotube is larger. This is also evident from Table 1, in which the local structure around the defect site for nanotubes containing SW defect is compared with a defect-free BC_3 nanotube. Compared with the perfect tube, the length of the bond shared by two heptagons (the central bond, d) increases for axial and decreases for circumferential bond rotations.

Table 1. Structural and Energetic Properties of SW Defects in BC_3 Nanotubes

system	central bond length (d) (Å)	reference bond length (Å)[a]	Θ_p (deg) for 1, 2 atoms	reference Θ_p values (deg)[a]	E_f (eV)
SW-CC-a	1.394	1.385	8.30, 8.52	7.22, 7.22	−0.10
SW-CC-c	1.334	1.412	2.80, 2.42	5.45, 7.22	2.67
SW-BC-a	1.563	1.501	7.53, 8.94	5.45, 6.91	−0.03
SW-BC-c	1.448	1.545	3.62, 2.02	6.91, 7.22	3.42

[a]Reference values are for the perfect nanotube.

The calculated pyramidalization angles (Θ_p) for the two atoms forming 7−7 junction (atoms 1 and 2 in Figure 2), as compared with the values for a perfect tube, are also presented in Table 1. The pyramidalization angle is a measure of the degree of sp^3 hybridization of an atom (or the deviation in the angle from that in a sp^2 hybrid), and is defined as ($\theta_{\sigma\pi}$ − 90°),

dx.doi.org/10.1021/jp303184q | J. Phys. Chem. C 2012, 116, 13225−13230

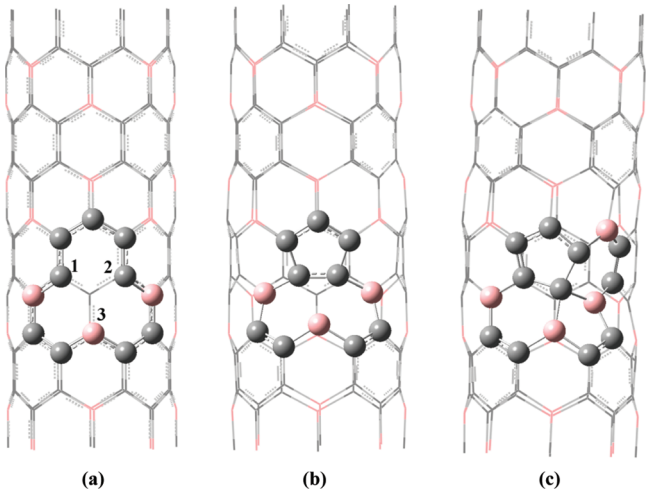

Figure 3. Carbon vacancy (V_C) in BC_3 nanotubes: (a) the initial structure with three dangling bonds (vc-3db), (b) a metastable structure with a new bond between 1, 2 atoms (vc-perp), and (c) the most stable structure obtained for V_C defect (vc-cross).

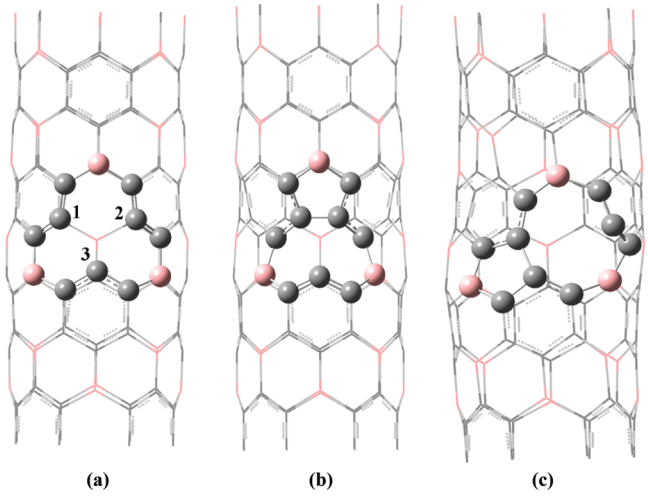

Figure 4. Boron vacancy (V_B) in BC_3 nanotubes: (a) a metastable structure with three dangling bonds (vb-3db), (b) a stable structure with a new bond between 1, 2 atoms (vb-perp), and (c) the most stable structure obtained for V_B defect (vb-para).

Table 2. Properties of BC_3 Nanotubes with Vacancy Defects

structure	E_f (eV)	μ_B	length of new bonds (Å)
vc-perp	2.49	0.00	1.446 (C−C)
vc-cross	1.13	0.00	1.470, 1.557 (C−C); 1.638, 1.595 (B−C)
vb-3db	5.42	1.00	
vb-perp	3.07	1.00	1.475 (C−C)
vb-para	2.62	1.00	1.571 (C−C)

in which $\theta_{\sigma\pi}$ is the angle between σ and π bonds. The values of Θ_p have been calculated using the Haddon's π-orbital axis vector (POAV) method.[24] For carbon atoms of curved polycyclic aromatic systems (such as nanotubes), the value of Θ_p is in the range of 0 (for trigonal planar geometries) to 19.5° (for tetrahedral structures). The magnitude of Θ_p has been shown to correlate with the local reactivity of atomic sites on the wall of single-walled carbon nanotubes (SWNTs).[25] For axial bond rotations (SW-CC-a and SW-BC-a), the atoms 1 and 2 in Figure 2 move outward from the nanotube's surface and

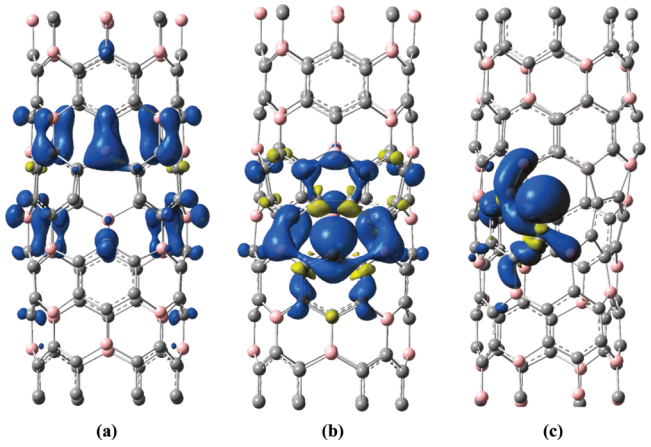

Figure 5. Spin-density isosurfaces for vb-3db (a), vb-perp (b), and vb-para (c) structures. Blue (dark) and yellow (light) regions correspond to positive and negative polarization, respectively. The isodensity value is 0.0015 μ_B/Bohr^3.

have pyramidalization angles of 7−9°, which are close to the corresponding angles for the perfect nanotube. For circumferential bond rotations, these atoms move inward and have lower Θ_p values. In accordance to relatively large values of Θ_p values for SW-CC-a and SW-BC-a systems, they have weaker central bonds (greater values of d), which means larger local reactivity.

The data in Table 1 show that for the SW-CC-a and SW-BC-a systems, the deviation of structural parameters from the defect-free state is lower than that of SW-CC-c and SW-BC-c systems; therefore, axial bond rotation produces more stable structures. This observation agrees with previous studies for CNTs[13,25] and BNNTs.[16] The positive bond length deviation for axial bond rotation and negative deviation for circumferential rotation has been observed in tight-binding calculations of CNTs,[13] but in calculations using other electronic structure methods[16,25] the bond length at 7−7 ring fusion always decreases with respect to the perfect tube.

We can also compare the stabilities using energy data. In Table 1, defect formation energies, defined as $E_f = E_{SW} - E_{perfect}$, are reported for various types of SW defects. For axial bond rotation, the defect formation energies have negative and small values, so that the defect can form spontaneously, leading to a stable structure. The formation of SW defects from a circumferential bond rotation has a greater energy "cost", which is reflected in their large and positive formation energies. Previous studies show that in CNTs and BNNTs, the axial bond rotation has a lower formation energy, but the values are always positive. The formation energies for SW defects in these systems are in the range of 4 to 5 eV,[13,16,25] which are greater than the values we have obtained for BC_3 nanotubes. The formation energies obtained by Zhao et al. for armchair BC_3 nanotubes are lower than the values for their corresponding CNTs.[18] However, they have only considered the bond rotation for a B−C bond perpendicular to the tube axis. Unlike the BNNTs,[16] the SW defect in a BC_3 nanotube does not form unstable homoelemental B−B bonds, and as a result, the structures are more stable.

In both -a and -c structures, CC bond rotation is more favorable than BC bond rotation, resulting in an overall stability order of SW-CC-a > SW-BC-a > SW-CC-c > SW-BC-c. Therefore, we conclude that the SW-CC-a structure is the most

dx.doi.org/10.1021/jp303184q | J. Phys. Chem. C 2012, 116, 13225−13230

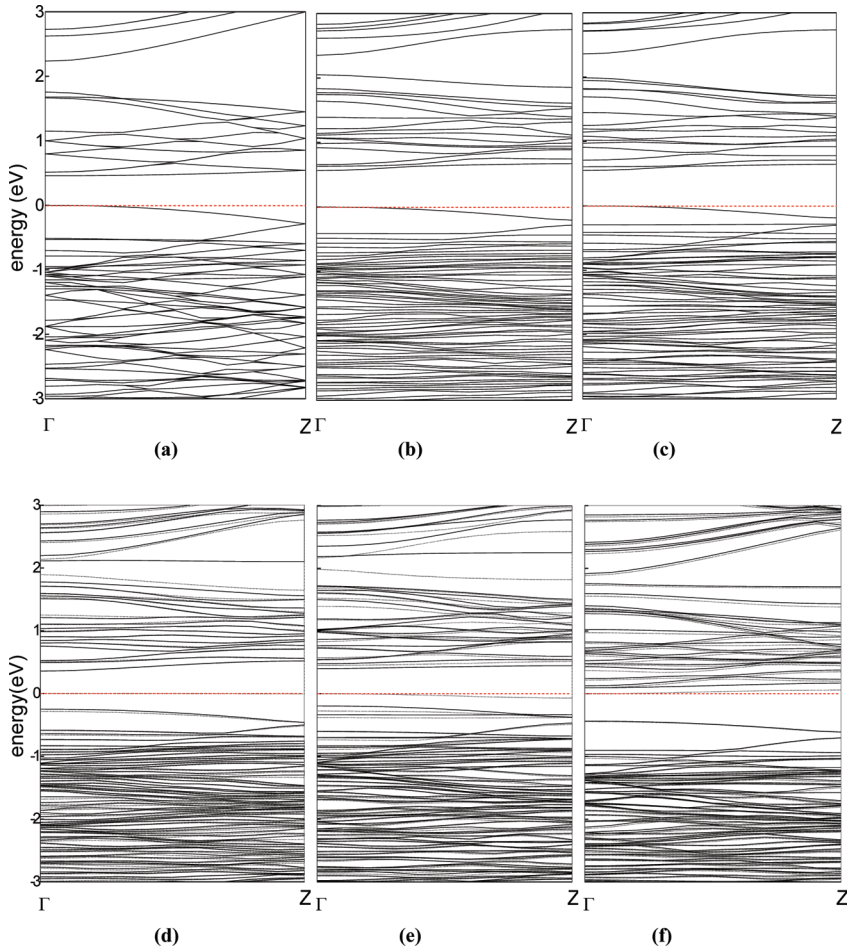

Figure 6. Electronic band structures for perfect (a), vc-cross (b), vc-perp (c), vb-para (d), vb-perp (e), and vb-3db (f) structures. Spin-up and spin-down bands are shown with dashed and solid lines, respectively. The dotted line indicates the position of the Fermi level.

stable BC_3 nanotube with a SW defect, with the lowest formation energy and minimum structural deformation with respect to the defect-free BC_3 nanotube.

B. Vacancy Defects. The effect of vacancy defects in BC_3 nanotubes is more complicated than that of Stone-Wales defects. When an atom is removed from the nanotube as a result of a vacancy defect, three sp^2-hybridized, two-coordinated atoms form around the defect position (atoms 1−3 in Figures 3a and 4a). The resulting structure in this "ideal vacancy" state is known as a structure with three dangling bonds (3db). The 3db structure is usually not stable and reconstructs in several ways.[26] One way is through the formation of a new bond between two undercoordinated atoms, leaving a five-membered ring and one dangling bond (5 + 1db structure). Because of the symmetry of a zigzag nanotube, two of the three under-coordinated atoms are equivalent (atoms 1 and 2 in Figures 3a and 4a). So, in a zigzag nanotube, there are two possible 5 + 1db structures, in which the new bond is perpendicular to the tube axis (1−2 bond) or in a tilted direction relative to it (either of two equivalent bonds 1−3 and 2−3). We denote these structures as "perpendicular" (or perp) and "parallel" (or para) systems, respectively.

To ensure that the most energetically stable structure has been identified rather than a structure corresponding to a local energy minimum, we examined several initial structures in addition to the ideal (or 3db) vacancy state. These include structures resembling parallel and perpendicular states, in which the atoms that are going to form a new bond are positioned closer to each other. Because vacancy defects may produce special defect states within the energy gap of semiconducting tubes, they can modify the electronic properties considerably. The presence of vacancies may lead to spin polarization near the defect site. As a result, spin-relaxed calculations have been used for all of these systems.

The defect formation energy for vacancies was obtained using the following expression

$$E_f = E_{defected} - E_{perfect} + \mu(X) \quad (1)$$

where $\mu(X)$ is the chemical potential of carbon (for V_C) or boron (for V_B) atom and is calculated as the total energy per atom in the crystal structure for the most stable form of that element. These structures are hexagonal 3D graphite with four C atoms and the rhombohedral structure of α-boron,[27] which has 12 B atoms. The calculation of chemical potentials was performed for one unit cell of graphite and α-boron, using a 7 × 7 × 7 grid of k-points and a kinetic energy cutoff of 350 eV. The defect formation energies obtained for vacancies in various structures are shown in Table 2.

For V_C defects, unconstrained optimization of all examined initial structures leads to the same minimum energy structure, which is shown in Figure 3c. In this structure, the system is reconstructed such that all dangling bonds are saturated and two pentagons and two hexagons form, having a common central atom, in a "cross" geometry (vc-cross). The cross

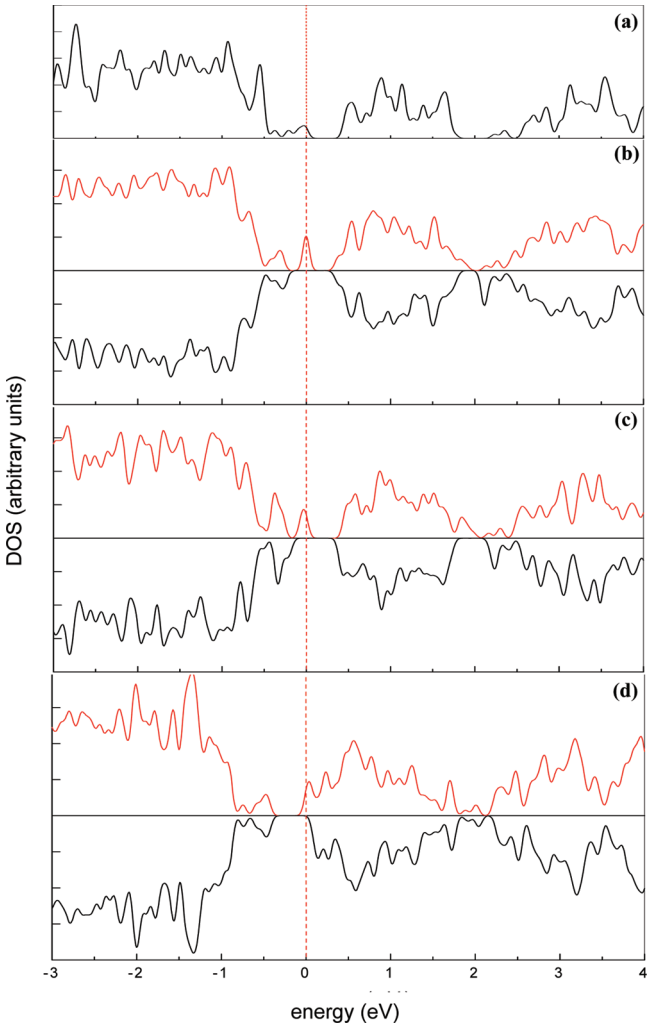

Figure 7. Total density of states (DOS) for perfect (a), vb-para (b), vb-perp (c), and vb-3db (d) systems. The dotted line indicates the position of the Fermi level. For defected systems, upper and lower panels are for spin-up and spin-down states, respectively.

structure has been observed as a stable but hard-to-reach state for zigzag nanotubes with a carbon vacancy.[15] A metastable structure for V_C, with an energy that is 10.7 meV/atom higher than the ground state, is a 5 + 1db structure, with the new bond perpendicular to tube axis (vc-perp). The length of the new bond is 1.446 Å, and its atoms move inward, whereas the undercoordinated atom moves outward with respect to the nanotube surface. The length of the new bond is lower than the values obtained for CNTs, which are ∼1.6 Å.[14,15] The defect formation energy for vc-cross is a bit lower than half the value for vc-perp, which means that the vc-cross structure is more likely to form than the vc-perp structure. The formation energies for carbon vacancy in CNTs are in the range of 4.5−8 eV, varying with the tube's chirality and the mode of reconstruction.[14,15,28]

It is evident in Table 2 that both of these structures are nonmagnetic. This is not unexpected for the vc-cross structure that has no dangling bonds, but in the case of vc-perp, the magnetic moment of the system is zero despite the presence of a two-coordinated atom. Similar behavior has been observed in some CNTs[15,28] and for V_C in SiC monolayers,[29] where it has been attributed to of structural distortions and electron transfer.

Structures obtained for a V_B defect are shown in Figure 4. The most stable structure is a 5 + 1db state, which is shown in Figure 4c. The new bond formed is almost parallel to the tube axis (vb-para), with a bond length that is larger than the value obtained for vc-perp. Another stable structure, with an energy that is 3.54 meV/atom higher, is vb-perp (Figure 4b), in which the new bond is between the values for vc-perp and vb-para. Another metastable structure is vb-3db (Figure 4a), with an energy difference of 22.1 meV/atom relative to the ground (vb-para) state. In this system, there are three dangling bonds, but atoms 1 and 2 move outside the plane of rings, and their distance increases to 2.91 Å relative to the ideal vacancy state. The 3db structure has been reported as a metastable structure for carbon vacancy in certain kinds of CNTs.[14,15,28] Table 2 shows that the vb-3db structure has the largest defect formation energy, but when a new bond is formed, the formation energy is lowered by a value that depends on the length (or strength) of the bond formed. Structures with shorter bond lengths have lower defect formation energies. This is consistent with the results obtained for CNTs.[15] In general, V_C defects have lower formation energies than V_B defects.

Unlike the case of carbon vacancies, the structures obtained for V_B defects all show a ferromagnetic ordering, with a net magnetic moment of 1.00 μ_B. Figure 5 shows the spin polarization for the structures shown in Figure 4. Both σ and π electrons contribute to spin polarization, and the magnetization is delocalized over a relatively large area around the defect. Note, however, that in vb-3db (Figure 5a) only one of the dangling bonds contributes in the spin polarization, resulting in a small magnetic moment of only 1.00 μ_B. However, for the vb-perp and vb-para structures, the magnetization comes mainly from the dangling bond, and, to a lesser extent, from the newly formed pentagon. The shape of spin-density isosurfaces resembles those obtained for CNTs with a carbon vacancy.[15]

Electronic band structures for the perfect BC_3 nanotube and the nanotubes with a carbon or boron vacancy are shown in Figure 6. The defect-free BC_3 nanotube is a semiconductor with a direct band gap of ∼0.5 eV between the highest valence band of σ character and the lowest conduction band, which has π character (Figure 6a). The calculated band gap agrees with previous DFT calculations.[9] This semiconductor behavior is preserved in the nanotubes with a V_C defect (Figure 6b,c). The Fermi level shifts slightly down as a result of fewer electrons, and the gap increases by only ∼0.1 eV. There is no specific "defect state" in the band structure of vc-perp and vc-cross.

In the case of V_B defects, the bands for spin-up and spin-down electrons are different, and there are additional defect states within the band gap, which are nearly flat. These flat bands are formed near the Fermi level as a result of vacancies that act like zigzag edges and interact via π electrons.[28]

The electronic structure of magnetic systems can be studied in more detail using total density of states (DOS) plots, which are shown in Figure 7 for perfect and BC_3 nanotubes with V_B defects. For the vb-para structure (Figure 7b), the band gap decreases, and a partially occupied defect state appears at the top of the valence band. The defect state is an acceptor state that may improve the conductivity at elevated temperatures. The same is true for the vb-perp structure (Figure 7c). The main contribution to the defect state for vb-para and vb-perp is from the undercoordinated atom, with some lower contributions from the atoms forming the new bond. For vb-3db (Figure 7d), the Fermi level shifts up and the defect state is a donor state in the bottom of the conduction band. This donor

dx.doi.org/10.1021/jp303184q | J. Phys. Chem. C 2012, 116, 13225−13230

state is composed of 2p atomic orbitals of only one of the undercoordinated atoms (atom 3 in Figure 4a). Hence, the dangling bond where the spin polarization is greatly localized is the main source of the defect state.

CONCLUSIONS

In this Article, we have studied the effect of Stone-Wales and vacancy defects on the structural and electronic properties of a (4, 0) BC_3 nanotubes. Compared with pure CNTs, the energetic cost of defect formation in BC_3 nanotubes is low for all types of defects studied, which implies that they are more likely to occur in such systems. Previous studies have shown that the effect of vacancies on the electronic properties of nanotubes depends strongly on the linear density (or concentration) of defects, the radius, and the chirality of the nanotube. Here the defects have been studied using BC_3 nanotubes of fixed length and radius, but the observations are in overall agreement with similar results for CNTs and BNNTs.

AUTHOR INFORMATION

Notes

The authors declare no competing financial interest.

ACKNOWLEDGMENTS

This work has been supported by the Iran National Science Foundation (INSF). Computations were performed on the GPC supercomputer at the SciNet HPC Consortium. SciNet is funded by: the Canada Foundation for Innovation under the auspices of Compute Canada; the Government of Ontario; Ontario Research Fund − Research Excellence; and the University of Toronto.

REFERENCES

(1) Kouvetakis, J.; Sasaki, T.; Chen, C.; Hagiwara, R.; Lerner, M.; Krishnan, K. M.; Bartlett, N. *Synth. Met.* **1989**, *34*, 1.
(2) Yao, B.; Chen, W. J.; Liu, L.; Ding, B. Z.; Su, W. H. *J. Appl. Phys.* **1998**, *84*, 1412.
(3) Azevedo, S.; de Paiva, R. *Europhys. Lett.* **2006**, *75*, 126.
(4) Weng-Sieh, Z.; Cherrey, K.; Chopra, N. G.; Blase, X.; Miyamoto, Y.; Rubio, A.; Cohen, M. L.; Louie, S. G.; Zettl, A.; Gronsky, R. *Phys. Rev. B* **1995**, *51*, 11229.
(5) Miyamoto, Y.; Rubio, A.; Louie, S. G.; Cohen, M. L. *Phys. Rev. B* **1994**, *50*, 18360.
(6) Carroll, D. L.; Redlich, Ph.; Blase, X.; Charlier, J.-C.; Curran, S.; Ajayan, P. M.; Roth, S.; Rühle, M. *Phys. Rev. Lett.* **1998**, *81*, 2332.
(7) Fuentes, G. G.; Borowiak-Palen, E.; Knupfer, M.; Pichler, T.; Fink, J.; Wirtz, L.; Rubio, A. *Phys. Rev. B* **2004**, *69*, 245403.
(8) Hernández, E.; Goze, C.; Bernier, P.; Rubio, A. *Phys. Rev. Lett.* **1998**, *80*, 4502.
(9) Kim, Y.-H.; Sim, H.-S.; Chang, K. J. *Curr. Appl. Phys.* **2001**, *1*, 39.
(10) Kim, Y.-H.; Chang, K. J.; Louie, S. G. *Phys. Rev. B* **2001**, *63*, 205408.
(11) Nardelli, M. B.; Yakobson, B. I.; Bernholc, J. *Phys. Rev. B* **1998**, *57*, 4277.
(12) Stone, A. J.; Wales, D. J. *Chem. Phys. Lett.* **1986**, *128*, 501.
(13) Pan, B. C.; Yang, W. S.; Yang, J. *Phys. Rev. B* **2000**, *62*, 12652.
(14) Orellana, W.; Fuentealba, P. *Surf. Sci.* **2006**, *600*, 4305.
(15) Berber, S.; Oshiyama, A. *Physica B* **2006**, *376*−*377*, 272.
(16) Li, Y.; Zhou, Z.; Golberg, D.; Bando, Y.; Schleyer, P. V. R.; Chen, Z. *J. Phys. Chem. C* **2008**, *112*, 1365.
(17) Piquini, P.; Baierle, R. J.; Schmidt, T. M.; Fazzio, A. *Nanotechnology* **2005**, *16*, 827.
(18) Guo, X.; Liao, J.; Zhao, J. *Nanotechnology* **2007**, *18*, 105705.
(19) Zhao, J.; Wen, B.; Zhou, Z.; Chen, Z.; Schleyer, P. V. R. *Chem. Phys. Lett.* **2005**, *415*, 323.
(20) Vanderbilt, D. *Phys. Rev. B* **1990**, *41*, 7892.
(21) Giannozzi, P.; Baroni, S.; Bonini, N.; Calandra, M.; Car, R.; Cavazzoni, C.; Ceresoli, D.; Chiarotti, G. L.; Cococcioni, M.; Dabo, I.; Dal Corso, A.; Fabris, S.; Fratesi, G.; de Gironcoli, S.; Gebauer, R.; Gerstmann, U.; Gougoussis, C.; Kokalj, A.; Lazzeri, M.; Martin-Samos, L.; Marzari, N.; Mauri, F.; Mazzarello, R.; Paolini, S.; Pasquarello, A.; Paulatto, L.; Sbraccia, C.; Scandolo, S.; Sclauzero, G.; Seitsonen, A. P.; Smogunov, A.; Umari, P.; Wentzcovitch, R. M. *J. Phys.: Condens. Matter* **2009**, *21*, 395502.
(22) Perdew, J. P.; Burke, K.; Ernzerhof, M. *Phys. Rev. Lett.* **1996**, *77*, 3865.
(23) Monkhorst, H. J.; Pack, J. D. *Phys. Rev. B* **1976**, *13*, 5188.
(24) Haddon, R. C. *J. Phys. Chem. A* **2001**, *105*, 4164.
(25) Dinadayalane, T. C.; Leszczynski, J. *Chem. Phys. Lett.* **2007**, *434*, 86.
(26) Ajayan, P. M.; Ravikumar, V.; Charlier, J.-C. *Phys. Rev. Lett.* **1998**, *81*, 1437.
(27) Decker, B. F.; Kasper, J. S. *Acta Crystallogr.* **1959**, *12*, 503.
(28) Ma, Y.; Lehtinen, P. O.; Foster, A. S.; Nieminen, R. M. *New J. Phys.* **2004**, *6*, 68.
(29) He, X.; He, T.; Wang, Z.; Zhao, M. *Physica E* **2010**, *42*, 2451.